Superlattices and Microstructures 143 (2020) 106556

Contents lists available at ScienceDirect

Superlattices and Microstructures

journal homepage: www.elsevier.com/locate/superlattices

Preparation of vertically aligned GaN@Ga_2O_3 core-shell heterostructured nanowire arrays and their photocatalytic activity for degradation of Rhodamine B

Liying Zhang, Yuewen Li, Xiangqian Xiu *, Guoqing Xin, Zili Xie, Tao Tao, Bin Liu, Peng Chen, Rong Zhang **, Youdou Zheng

Key Laboratory of Advanced Photonic and Electronic Materials, School of Electronic Science and Engineering, Nanjing University, Nanjing, 210023, Jiangsu, PR China

ARTICLE INFO

Keywords:
GaN
Ga_2O_3
Core-shell structure
Nanowire arrays
Photocatalytic activity
Rhodamine B

ABSTRACT

In this paper, vertically aligned GaN@Ga_2O_3 core-shell heterostructured nanowire arrays have been fabricated by thermal oxidation of GaN nanowire arrays. GaN nanowire arrays have been prepared by inductively coupled plasma etching. The GaN@Ga_2O_3 nanowire arrays have the good morphology and the thickness of the Ga_2O_3 shell can be controlled by the oxidation duration and temperature. The photocatalytic activity of vertically aligned GaN@Ga_2O_3 nanowires has been first evaluated by the degradation of Rhodamine B solution. Compared with the original GaN nanowires and the oxidized Ga_2O_3 nanowires, GaN@Ga_2O_3 nanowires exhibit superior photocatalytic activity. This finding suggests that GaN nanowire arrays with enhanced photocatalytic activity could be obtained by construct heterostructured GaN-based nanocomposite, which provides a new possibility for photocatalytic applications.

1. Introduction

Semiconductor nanomaterials have a wide range of applications due to their one-dimension structure, large surface-to-volume ratio and light-trapping ability [1–5]. Among numerous nanomaterials, GaN (E_g = 3.4 eV) and Ga_2O_3 (E_g = 4.8–4.9 eV) have attracted tremendous attention because of their wide bandgap, good chemical and thermal stability, and favorable optical and electric properties [6–10]. Recently, extensive efforts have been made on GaN-Ga_2O_3 nanocomposite materials because the unique heterostructure provides a variety of novel functions not originally available in either GaN or Ga_2O_3 nanostructures [11–18]. GaN@Ga_2O_3 core-shell nanowires (NWs) are a case in point.

On the other hand, both GaN and Ga_2O_3 are promising photocatalytic materials due to their excellent chemical stability and being capable to photo-oxidative destruction of organic dyeing pollutants [19–22]. Similar with other semiconductor nanocomposites, GaN@Ga_2O_3 core-shell nanocomposites are expected to improve photocatalytic activity [23–26]. However, there are few reports of GaN@Ga_2O_3 core-shell nanocomposites to enhance photocatalytic efficiency [11]. In addition, photocatalytic applications of the vertically aligned GaN@Ga_2O_3 core-shell nanowire arrays (NAs) has not been reported so far.

For the preparation of GaN@Ga_2O_3 NWs, current researches have employed two main methods. i) Synthesis of the GaN@Ga_2O_3

* Corresponding author.
** Corresponding author.
E-mail addresses: xqxiu@nju.edu.cn (X. Xiu), rzhang@nju.edu.cn (R. Zhang).

https://doi.org/10.1016/j.spmi.2020.106556
Received 26 January 2020; Received in revised form 26 April 2020; Accepted 3 May 2020
Available online 7 May 2020

core-shell NWs by hetero-epitaxy [12,13]. ii) Introduction of the Ga_2O_3 outer shell via thermal oxidation of the GaN core [16–18]. Among them, thermal oxidation is a preferable method with simple operation and low cost. However, most reported GaN@Ga_2O_3 core-shell nanowires are inclined or planar. As widely known, the inductively coupled plasma (ICP) etching is a simple and feasible approach to fabricate vertically aligned GaN NAs [27–29]. In this paper, we have prepared the vertically aligned GaN@Ga_2O_3 core-shell heterostructured NAs by thermally oxidizing GaN NAs fabricated via ICP etching.

The microstructure feature and the photocatalytic property for degrading Rhodamine B (RhB, $C_{28}H_{31}N_2O_3Cl$) of the GaN@Ga_2O_3 core-shell NAs have been first investigated. And the possible mechanism of the enhanced catalysis of GaN@Ga_2O_3 core-shell NAs for the photodegradation of RhB has been discussed.

2. Experimental details

The well-aligned GaN NAs were first fabricated by ICP etching using self-organized nickel nano-mask as the etching masks on GaN/sapphire (the experimental details were described in Ref. [28]). Then the GaN@Ga_2O_3 and Ga_2O_3 NAs were formed from the GaN NAs by controlling the thermal oxidation parameters. The oxidation process was carried out in an O_2 flow of 200 sccm at 850 °C for 15 min and at 1000 °C for 10 min, respectively. The microstructural features of the oxidized NAs were characterized by scanning electron microscopy (SEM), transmission electron microscopy (TEM) and energy dispersive spectroscope (EDS). In addition, the NAs samples oxidized at 900 °C for 10 min and at 950 °C for 5 min, 10min were also prepared to examine the effect of the oxidation parameters on the oxidized shell thickness. The photocatalytic experiments were conducted at room temperature under simulated sunlight irradiation by a 500 W Xe lamp. The RhB dye was chosen to study the photodegradation activity of NAs. All NAs samples on sapphire substrate ($1.5 \times 0.8\ cm^2$) were completely immersed in the aqueous solution containing 7.5 mg/L of RhB dye. The distance from the glass tube to light source was fixed at 10 cm and the irradiation time was 4 h. At hourly intervals, the solution was taken out and the degradation of RhB was determined by measuring the maximum absorbance at 526 nm on UV-6100S double beam spectrophotometer. The absorbance of the pure RhB without NAs was measured as a reference standard.

3. Results and discussions

3.1. Material characterization

Fig. 1a shows the schematic diagram for the fabrication of vertically aligned GaN@Ga_2O_3 core-shell heterostructured NAs. Fig. 1b and c show the tilted-view and cross-sectional (the insets) SEM images of the original GaN NAs and the oxidized GaN@Ga_2O_3 NAs at 850 °C. Both the samples exhibit a morphology of vertically aligned nanowires with a density of $6.4 \times 10^8/cm^2$. The average diameter and length of the original GaN NAs are ~0.21 μm and ~2 μm, respectively (Fig. 1b). After the oxidation, the NAs can still maintain the original morphology but the surface of obtained GaN@Ga_2O_3 NAs is roughened (Fig. 1c). The rougher surface means the large surface-to-volume ratio, which can provide trap sites of carriers in novel device application.

Fig. 2a shows the TEM image of a typical GaN@Ga_2O_3 core-shell nanowire oxidized at 850 °C for 15 min. The single nanowire

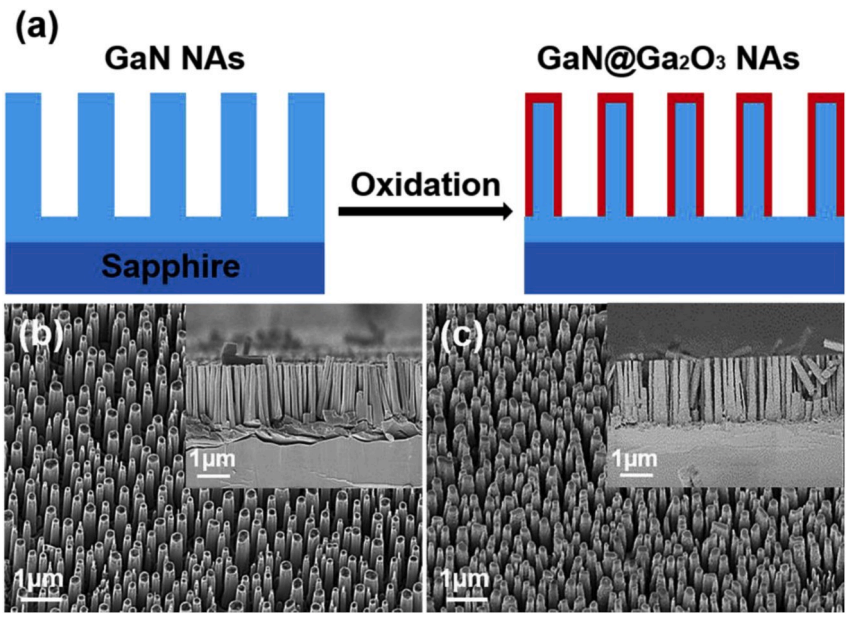

Fig. 1. (a) Schematic diagram of the fabrication of GaN@Ga_2O_3 core-shell nanowire arrays. Tilted-view and cross-sectional SEM images of (b) the original GaN NAs and (c) the GaN@Ga_2O_3 NAs oxidized at 850 °C for 15 min.

exhibits a uniform core-shell morphology, and the thickness of Ga_2O_3 shell is estimated as ~5 nm. It suggests that the oxidation rate is uniform along the radial directions of the nanowire. Fig. 2b shows the high-resolution TEM image near the GaN@Ga_2O_3 interface. Two regions are marked: (A) the GaN core and (B) the Ga_2O_3 shell. The inset of Fig. 2b shows a selected area electron diffraction (SAED) pattern in the interface, which include the hexagonal spotty diffraction pattern from [0002] direction of GaN and a discontinuous ring with discrete spots from Ga_2O_3 shell. The clear lattice fringes are obviously observed and the interplanar spacing of GaN (0002) is calculated to be 0.255 nm in region A (Fig. 2c). In region B, the Ga_2O_3 shell consists of large grains, and the interplanar spacing of Ga_2O_3 (400) is 0.307 nm (Fig. 2d). The above results indicate that the core of nanowire is single-crystal wurtzite GaN and the shell is polycrystalline Ga_2O_3. In addition, the EDS spectra have been conducted by line-scanning and mapping to determine the elemental distributions along the core-shell nanowire (Fig. 2e and f). It can be found that the GaN nanowire is homogeneously wrapped in the 5-nm thick Ga_2O_3 shell, which are in agreement with the TEM result.

The effect of the oxidation conditions on the shell thickness of core-shell NAs has been studied, the shell thickness increases with increasing the temperature and the oxidation time as shown in Fig. 3a. After oxidation at 1000 °C for 10 min, the vertically aligned GaN NAs have been completely converted to vertically aligned Ga_2O_3 NAs with rougher surface (Fig. 3b–d). The average diameter of Ga_2O_3 NAs increases slightly to ~0.22 μm (Fig. 3b). The HRTEM image indicates that the high temperature oxidation improves the crystallinity of Ga_2O_3 NAs, shown in Fig. 3d.

3.2. Photocatalytic activity and stability

The photocatalytic activities of original GaN NAs, GaN@Ga_2O_3 core-shell NAs (850 °C, 15min) and Ga_2O_3 NAs (1000 °C, 10min) have been investigated by the degradation of RhB under simulated sunlight illumination. Fig. 4 shows the corresponding degradation UV–visible spectra of RhB solution. Blank test (Fig. 4a) shows that the RhB solution is slowly self-degraded over the irradiation time and around 49% of RhB is remained after 3 h. Photocatalytic experiments (Fig.4b–d) clearly demonstrate that GaN@Ga_2O_3 NAs exhibit better photocatalytic activity compared with pure GaN and Ga_2O_3 NAs. After 3 h irradiation, the maximum absorption peak of RhB almost vanishes for GaN@Ga_2O_3 (Fig. 4c) NAs, while it still exists for the pure GaN (Fig. 4b) and Ga_2O_3 (Fig. 4d) NAs. In order to observe the result of photocatalytic degradation directly, the photograph of different samples is shown in Fig. 4e. Among all the samples, it can be found that GaN@Ga_2O_3 NAs show the best photocatalytic activity.

The degradation efficiency (D) of RhB can be calculated by $D = (1 - A/A_0) \times 100\%$, where A_0 is the initial absorbance of the RhB solution without treatment and A is the absorbance after reaction [30]. To better distinguish the photocatalytic activities of these samples, the degradation efficiency of RhB is plotted in Fig. 5a. After 3 h irradiation, the degradation efficiency is about 51%, 81%, 93% and 81% for pure RhB, GaN, GaN@Ga_2O_3 and Ga_2O_3 NAs, respectively. In addition, the photocatalytic degradation reaction of RhB follows the pseudo-first-order reaction equation $ln(C_0/C) = kt$ [20], and the apparent rate constant (k) reflects the degradation rate of RhB under sunlight irradiation. As shown in Fig. 5b, the derived k values are 0.0042 min^{-1}, 0.0094 min^{-1}, 0.0142 min^{-1}, and 0.0096 min^{-1} for pure RhB, GaN, GaN@Ga_2O_3 and Ga_2O_3 NAs, respectively. The order of rate constants is summarized as follows: GaN@Ga_2O_3 > Ga_2O_3 > GaN > RhB, which is consistent with the conclusions of photocatalytic degradation curves presented in Fig. 5a. These results suggest that construction of GaN@Ga_2O_3 core-shell structure is beneficial to enhance the photocatalytic performance.

As the stability of a photocatalyst is very important for its practical applications, three successive cyclic photocatalytic degradation

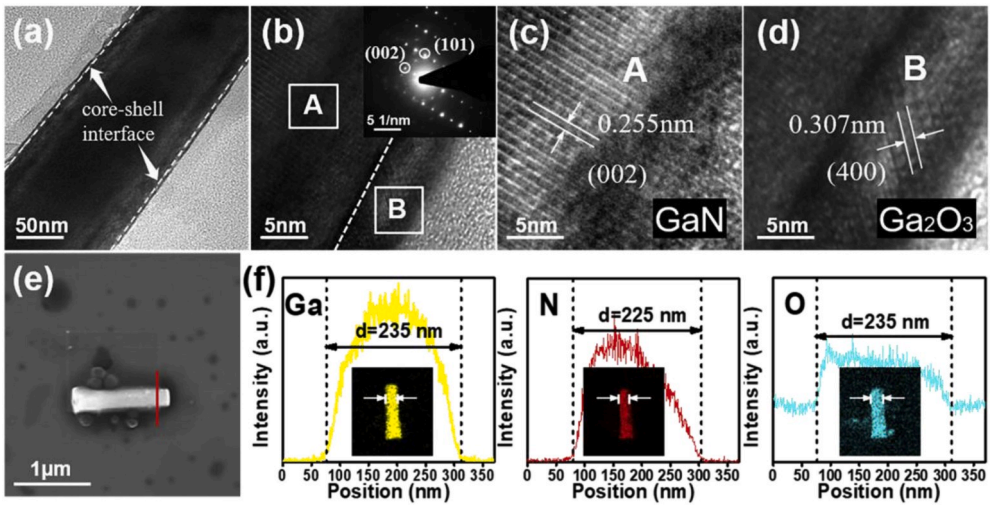

Fig. 2. (a) TEM image of a GaN@Ga_2O_3 core-shell nanowire oxidized at 850 °C for 15 min. HRTEM images of the core-shell nanowire: (b) the core-shell interface, (c) GaN core and (d) Ga_2O_3 shell. The inset of (b) is the diffraction pattern taken at the interface. (e) The SEM graph of a GaN@Ga_2O_3 core-shell nanowire. (f) The EDS nanoprobe line-scan for the elements Ga, N and O along the red line in (d) and the corresponding EDS elemental mappings.

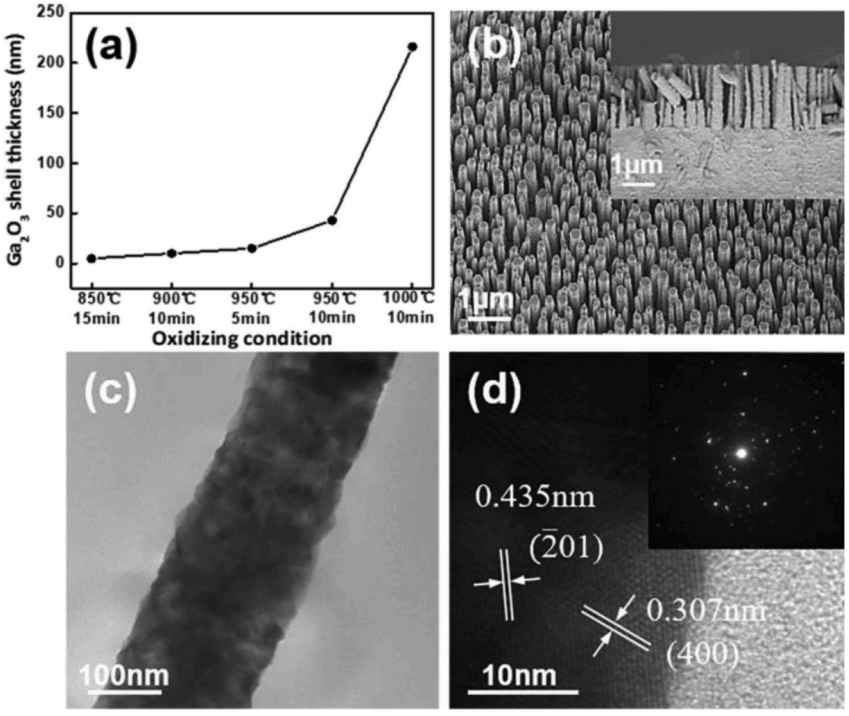

Fig. 3. (a) The variation of the Ga_2O_3 shell thickness under different oxidation conditions. (b) Tilted-view SEM, (c) TEM and (d) HRTEM images of the oxidized Ga_2O_3 NAs from GaN at 1000 °C. The inset of (b) is the cross-sectional SEM image of the Ga_2O_3 NAs and the inset of (d) is the diffraction pattern.

tests have been performed to investigate the stability and reusability of GaN@Ga_2O_3 NAs. As shown in Fig. 5c, the degradation rates of RhB show only a slight decrease after three cycles, indicating that GaN@Ga_2O_3 NAs can be used as a stable photocatalyst.

3.3. Photocatalytic mechanism

Under irradiation, the NAs can absorb light to generate electron-hole pairs. The photogenerated electrons (e^-) react with the dissolved O_2 molecules in water to yield the highly oxidative species like superoxide radical anions ($O_2^{\bullet-}$), which on protonation generate hydroperoxyl radicals ($HO_2^{\bullet}$), and eventually produce hydroxyl radical ($OH^{\bullet}$). Meanwhile, the photogenerated holes (h^+) could potentially react with the surface water molecule to form highly reactive hydroxyl radical ($OH^{\bullet}$). The hydroxyl radical ($OH^{\bullet}$) is a strong oxidizing agent to degrade the organic RhB dye. The photogenerated holes themselves can also directly oxidize the organic dye. The above possible reactions for the degradation of RhB are listed as follows:

$$e^- + O_2 \rightarrow O_2^{\bullet-} \quad (1)$$

$$O_2^{\bullet-} + H_2O \rightarrow HO_2^{\bullet} + OH^- \quad (2)$$

$$HO_2^{\bullet} + H_2O \rightarrow H_2O_2 + OH^{\bullet} \quad (3)$$

$$H_2O_2 \rightarrow 2OH^{\bullet} \quad (4)$$

$$h^+ + H_2O \rightarrow OH^{\bullet} + H^+ \quad (5)$$

$$OH^{\bullet}/O_2^{\bullet-}/h^+ + RhB \rightarrow CO_2 + H_2O + micromolecules \quad (6)$$

So the photogenerated electron-hole pairs by UV irradiating NAs enhance the photodegradation of RhB dye. Although the bandgap of Ga_2O_3 (4.8–4.9 eV) is bigger than that of GaN (3.4 eV), the photodegradation efficiency of Ga_2O_3 NAs is slightly higher than that of GaN NAs, which may be due to their increased surface area after the oxidation. The surface area of Ga_2O_3 NAs increases by about 5% after the complete conversion from GaN NAs, which increases the contact area with the RhB solution. GaN@Ga_2O_3 exhibit higher photocatalytic activity than that of pure GaN and Ga_2O_3 NAs. On the one hand, the novel core-shell structure increases the absorption of light with different wavelengths, and on the other hand, the core-shell heterostructured structure can accelerate the separation of photogenerated charge carriers which is similar to those that have been well reported in the literature [23–25].

Compared with other GaN/Ga_2O_3 based nanowires photocatalysts reported previously, GaN@Ga_2O_3 NAs can achieve comparable or superior photocatalytic efficiency with smaller surface area [20–22]. Table 1 shows the comparison of the photodegradation

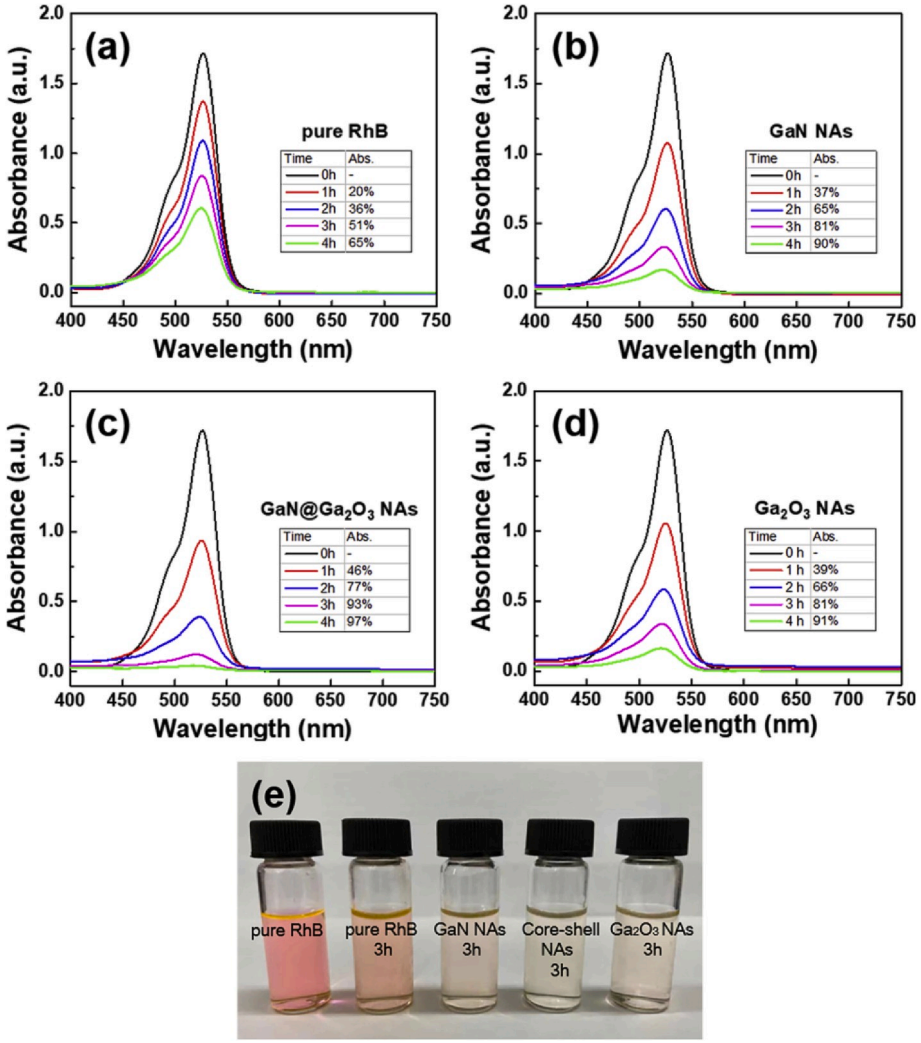

Fig. 4. Time-dependent UV–visible spectra of RhB solution (a) without photocatalyst and with (b) GaN NAs, (c) GaN@Ga_2O_3 NAs, and (d) Ga_2O_3 NAs. (e) Photographs of the original RhB solution and the degraded RhB solutions after 3 h irradiation.

parameters of present GaN/Ga_2O_3 based nanowires photocatalysts.

4. Conclusions

In conclusion, we have fabricated vertically aligned GaN@Ga_2O_3 core-shell heterostructured NAs by thermal oxidizing GaN NAs prepared by ICP etching. SEM and TEM observations verify that the prepared GaN@Ga_2O_3 nanowire owns uniform core-shell structure. The well-ordered core-shell NAs with controllable shell thickness have been demonstrated. Compared with pure GaN and Ga_2O_3 NAs, GaN@Ga_2O_3 NAs shows the better photocatalytic activity for the degradation of Rhodamine B. These results indicate that the combination of ICP etching and oxidation is a simple and practicable way to realize the vertically aligned GaN@Ga_2O_3 NAs, and the core-shell NAs is a promising candidate for photocatalytic applications.

Declaration of competing interests

The authors declare that they have no known competing financial interests or personal relationships that could have appeared to influence the work reported in this paper.

CRediT authorship contribution statement

Liying Zhang: Conceptualization, Investigation, Writing - original draft. **Yuewen Li:** Resources, Validation. **Xiangqian Xiu:**

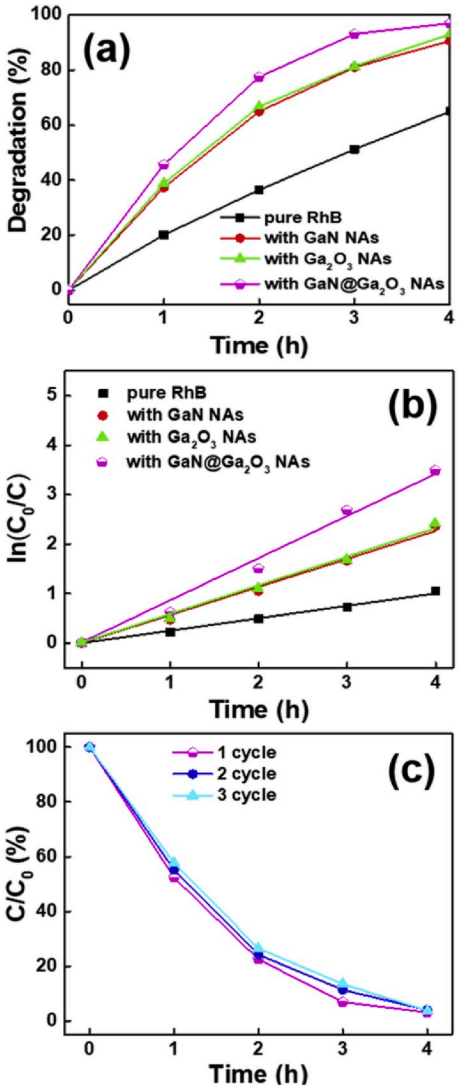

Fig. 5. (a) Degradation profiles and (b) kinetic liner simulation curves of RhB photocatalytic degradation without catalyst and with GaN, GaN@Ga_2O_3 and Ga_2O_3 NAs. (c) Photocatalytic stability of the GaN@Ga_2O_3 NAs for RhB photodegradation with three cycles of use.

Table 1
Comparison of the photodegradation parameters for GaN/Ga_2O_3 based nanowires photocatalysts.

Catalyst	Structure	Nanostructure dimension	Density	Pollutant	Degradation	*k*	Ref.
GaN NWs	inclined	D:0.12 μm, L:10 μm	–	MB	93% (4 h)	–	[20]
GaN NAs	vertically aligned	D:0.21 μm, L:2 μm	$6.4 \times 10^8/cm^2$	RhB	81% (3 h)	0.0094 min^{-1}	this work
Ga_2O_3 Nanobelts	inclined	D:>0.09 μm, L:10–40 μm	–	RhB/MB	70%/93% (2 h)	0.0087/0.0142 min^{-1}	[21]
Ga_2O_3 Nanorods	parallely aligned	D:0.05 μm, L:200 μm	1000 mg/L	RhB	92% (3 h)	–	[22]
Ga_2O_3 NAs	vertically aligned	D:0.22 μm, L:2 μm	$6.4 \times 10^8/cm^2$	RhB	81% (3 h)	0.0096 min^{-1}	this work
GaN@Ga_2O_3 NAs	vertically aligned	D:0.21 μm, L:2 μm	$6.4 \times 10^8/cm^2$	RhB	93% (3 h)	0.0142 min^{-1}	this work

Note: D, nanowire diameter; L, nanowire length; MB, Methylene Blue.

Conceptualization, Supervision, Funding acquisition, Writing - review & editing. **Guoqing Xin:** Resources, Validation. **Zili Xie:** Resources, Validation. **Tao Tao:** Resources, Validation. **Bin Liu:** Resources, Validation. **Peng Chen:** Resources, Validation. **Rong Zhang:** Supervision, Funding acquisition. **Youdou Zheng:** Supervision, Funding acquisition.

Acknowledgements

This work is financially supported by the National Key R&D Program of China (2017YFB0404201), the State Key R&D Program of Jiangsu Province (BE2019103), the Six-Talent Peaks Project of Jiangsu Province (XCL-107), the Fund from the Solid-state Lighting and Energy-saving Electronics Collaborative Innovation Center, PAPD, and the Fund from the State Grid Shandong Electric Power Company.

References

[1] K. Peng, Y. Xu, Y. Wu, Y. Yan, S.T. Lee, J. Zhu, Aligned single-crystalline Si nanowire arrays for photovoltaic applications, Small 1 (11) (2005) 1062–1067.
[2] I.G. Valls, M.L. Cantu, Vertically-aligned nanostructures of ZnO for excitonic solar cells: a review, Energy Environ. Sci. 2 (2009) 19–34.
[3] F. Motahari, M.R. Mozdianfard, F. Soofivand, M.S. Niasari, NiO nanostructures: synthesis, characterization and photocatalyst application in dye pollution wastewater treatment, RSC Adv. 4 (52) (2014) 27654–27660.
[4] X. Zhang, X. Han, J. Su, Q. Zhang, Y. Gao, Well vertically aligned ZnO nanowire arrays with an ultra-fast recovery time for UV photodetector, Appl. Phys. A 107 (2012) 255–260.
[5] M.M. Kamazani, Z. Zarghami, M.S. Niasari, Facile and novel chemical synthesis, characterization, and formation mechanism of copper sulfide (Cu_2S, Cu_2S/CuS, CuS) nanostructures for increasing the efficiency of solar cells, J. Phys. Chem. C 120 (4) (2016) 2096–2108.
[6] S.T. Strite, H. Morkoc, GaN, AlN, and InN: a review, J. Vac. Sci. Technol. B 10 (4) (1992) 1237–1266.
[7] X. Duan, C.M. Lieber, Laser-assisted catalytic growth of single crystal GaN nanowires, J. Am. Chem. Soc. 122 (2000) 188–189.
[8] B.O. Jung, S.Y. Bae, Y. Kato, M. Imura, D.S. Lee, Y. Honda, H. Amano, Morphology development of GaN nanowires using a pulsed-mode MOCVD growth technique, CrystEngComm 16 (2014) 2273–2282.
[9] C.H. Liang, G.W. Meng, G.Z. Wang, Y.W. Wang, L.D. Zhang, Catalytic synthesis and photoluminescence of β-Ga_2O_3 nanowires, Appl. Phys. Lett. 78 (21) (2001) 3202–3204.
[10] S.J. Pearton, J. Yang, P.H. Cary IV, F. Ren, J. Kim, M.J. Tadjer, M.A. Mastro, A review of Ga_2O_3 materials, processing, and devices, Appl. Phys. Rev. 5 (2018), 011301.
[11] H.D. Xiao, H.Y. Pei, J.Q. Liu, J.S. Cui, B. Jiang, Q.J. Hou, W.R. Hu, Fabrication, characterization, and photocatalysis of GaN-Ga_2O_3 core-shell nanoparticles, Mater. Lett. 71 (2012) 145–147.
[12] S. Lee, M.H. Ham, J.M. Myoung, W. Lee, Epitaxial synthesis of GaN/Ga_2O_3 core/shell nanocable heterostructures by atmosphere control, Acta Mater. 58 (2010) 4714–4722.
[13] Y.K. Lee, H. Medina, P.W. Chiu, Modifying optical properties of GaN nanowires by Ga_2O_3 overgrowth, J. Vac. Sci. Technol. B 30 (1) (2012), 011802.
[14] M. Kumar, G. Sarau, M. Heilmann, S. Christiansen, V. Kumar, R. Singh, Effect of ammonification temperature on the formation of coaxial GaN/Ga_2O_3 nanowires, J. Phys. D Appl. Phys. 50 (2017), 035302.
[15] Y. Li, Z. Xiong, D. Zhang, X. Xiu, D. Liu, S. Wang, X. Hua, Z. Xie, T. Tao, B. Liu, P. Chen, R. Zhang, Y. Zheng, Study of GaN nanorods converted from β-Ga_2O_3, Superlattice. Microst. 117 (2018) 235–240.
[16] C.C. Tang, Y. Bando, Z.W. Liu, Thermal oxidation of gallium nitride nanowires, Appl. Phys. Lett. 83 (15) (2003) 3177.
[17] M.H. Ham, S. Lee, J.M. Myoung, W. Lee, Controlled formation of oxide shells from GaN nanowires: poly- to single-crystal, Electron. Mater. Lett. 7 (3) (2011) 243–247.
[18] S. Wang, Y.W. Li, X.Q. Xiu, L.Y. Zhang, X.M. Hua, Z.L. Xie, T. Tao, B. Liu, P. Chen, R. Zhang, Y.D. Zheng, Synthesis and characterization of β-Ga_2O_3@GaN nanowires, Chin. Phys. B 28 (2) (2019), 02814.
[19] H.S. Jung, Y.J. Hong, Y. Li, J. Cho, Y.J. Kim, G.C. Yi, Photocatalysis using GaN nanowires, ACS Nano 2 (4) (2008) 637–642.
[20] V. Purushothaman, S. Prabhu, K. Jothivenkatachalam, S. Parthiban, J.Y. Kwon, K. Jeganathan, Photocatalytic dye degradation properties of wafer level GaN nanowires by catalytic and self-catalytic approach using chemical vapor deposition, RSC Adv. 4 (49) (2014) 25569.
[21] L.C. Tien, W.T. Chen, C.H. Ho, Enhanced photocatalytic activity in β-Ga_2O_3 nanobelts, J. Am. Ceram. Soc. 94 (9) (2011) 3117–3122.
[22] K. Girija, S. Thirumalairajan, D. Mangalaraj, Morphology controllable synthesis of parallely arranged single-crystalline β-Ga_2O_3 nanorods for photocatalytic and antimicrobial activities, Chem. Eng. J. 236 (2014) 181–190.
[23] S. Khanchandani, S. Kundu, A. Patra, A.K. Ganguli, Shell-thickness dependent photocatalytic properties of ZnO/CdS core-shell nanorods, J. Phys. Chem. C 116 (2012) 23653–23662.
[24] X. Qu, D. Xie, L. Gao, F. Du, Synthesis and characterization of TiO_2/ZrO_2 coaxial core-shell composite nanotubes for photocatalytic applications, Ceram. Int. 40 (8B) (2014) 12647–12653.
[25] H.R. Liu, C.J. Hu, H.F. Zhai, J. Yang, X.G. Liu, H.S. Jia, Fabrication of In_2O_3/ZnO@Ag nanowire ternary composites with enhanced visible light photocatalytic activity, RSC Adv. 7 (59) (2017) 37220–37229.
[26] Y. Chen, S. Li, R.Y. Zhao, W. Li, Z.H. Ren, G.R. Han, Single-crystal TiO_2/$SrTiO_3$ core–shell heterostructured nanowire arrays for enhanced photoelectrochemical performance, Rare Met. 38 (5) (2019) 369–378.
[27] C.C. Yu, C.F. Chu, J.Y. Tsai, H.W. Huang, T.H. Hsueh, C.F. Lin, S.C. Wang, Gallium nitride nanorods fabricated by inductively coupled plasma reactive ion etching, Jpn. J. Appl. Phys. 41 (8B) (2002) L910–L912.
[28] Z.Q. Lin, X.Q. Xiu, S.Y. Zhang, X.M. Hua, Z.L. Xie, R. Zhang, P. Han, Y.D. Zheng, Arrays of GaN nano-pillars fabricated by nickel nano-island mask, Mater. Lett. 108 (2013) 250–252.
[29] F. Yu, S. Yao, F. Römer, B. Witzigmann, T. Schimpke, M. Strassburg, A. Bakin, H.W. Schumacher, E. Peiner, H.S. Wasisto, A. Waag, GaN nanowire arrays with nonpolar sidewalls for vertically integrated field-effect transistors, Nanotechnology 28 (2017), 095206.
[30] S.M. Derazkola, S.Z. Ajabshir, M.S. Niasari, Novel simple solvent-less preparation, characterization and degradation of the cationic dye over holmium oxide ceramic nanostructures, Ceram. Int. 41 (2015) 9593–9601.